Relativistic and QED effects on NMR magnetic shielding constant of neutral and ionized atoms and diatomic molecules[a)]

Karol Kozioł,[1,2,b)] I. Agustín Aucar,[1,3,c)] and Gustavo A. Aucar[1,3,d)]
[1)] *Institute for Modelling and Innovative Technology, IMIT, Corrientes, Argentina*
[2)] *Narodowe Centrum Badań Jądrowych (NCBJ), Andrzeja Sołtana 7, 05-400 Otwock-Świerk, Poland*
[3)] *Physics Department, Natural and Exact Science Faculty, Northeastern University of Argentina, Corrientes, Argentina*

(Dated: 4 April 2019)

We show here results of four-component calculations of NMR σ for atoms with $10 \leq Z \leq 86$ and their ions, within the polarization propagator formalism at its random phase level of pproach, and the first estimation of QED effects and Breit interactions of those atomic systems by using two theoretical effective models. We also show QED corrections to $\sigma(X)$ in simple diatomic HX and X_2 (X = Br, I, At) molecules. We found that the Z dependence of QED corrections in bound-state many-electron systems is proportional to Z^5, which is higher than its dependence in H-like systems. The analysis of relativistic ee (or paramagnetic-like) and pp (or diamagnetic-like) terms of σ, expose two different patterns: the pp contribution arise from virtual electron-positron pair creation/annihilation, and the ee contribution is mainly given by $1s \rightarrow ns$ and $2s \rightarrow ns$ excitations. The QED effects on shieldings have a negative sign and their magnitude is larger than 1% of the relativistic effects for high-Z atoms like Hg and Rn, and up to 0.6% of its total four-component value for neutral Rn. Furthermore, percentual contributions of QED effects to the total shielding are larger for ionized than for neutral atoms. In molecule, the contribution of QED effects to $\sigma(X)$ is determined by its highest-Z atoms, being up to -0.6% of its total σ value for astatine compounds. It is found that QED effects grow faster than relativistic effects with Z.

Keywords: Relativistic effects, ee and pp contributions, diatomic molecules

I. INTRODUCTION

Nuclear magnetic resonance (NMR) spectroscopy is a powerful experimental technique used, among many other applications, to identify chemical compounds and predict their molecular structures. Precise calculations of both of its relevant spectroscopic parameters, the NMR shielding constant, σ, and the J-coupling (indirect spin-spin coupling) constant, are highly challenging. They require to consider several intra- and intermolecular effects with the proper theories and state-of-the-art models.[1–4]

There are few leading electronic effects, such as the electron correlation and relativistic effects, that should be included in order to get an accurate theoretical reproduction of the nuclear magnetic shieldings. In the case of heavy-atom containing molecules it is known that relativistic effects may be as large as the non-relativistic (NR) contributions.[5,6] Furthermore, it was recently shown that electron correlation effects within a four-component DFT scheme and relativistic effects may not be independent each other, for NMR spectroscopic parameters.[6,7] When one looks for the most accurate results, the effects of the nuclear size and quantum electrodynamic (QED) corrections must be included.[8,9] The nuclear charge distribution effects on shieldings may be of the order 3% to 6% in heavy-atom containing molecules as HAt and $PbIH_3$.[7,10]

The first theoretical models developed to introduce QED effects (the self-energy part) on σ, were presented by Romero and Aucar.[11,12] In those models the main difficulties were related with solutions of formal expressions and implementations, like the integrals for the fourth level of the scattering matrix. During the last couple of years few attempts were made to estimate quantitatively the influence of QED effects on shielding of H-like and He-like systems.[13–15] Rudziński *et al.*[13] have published relativistic and QED corrections to the shielding of ^{3}He, derived from the Breit-Pauli Hamiltonian. They concluded that QED corrections are non-negligible, being 1% of the relativistic contribution. These findings are in line with previous suggestions of Pyykkö and Zhao[16]. Afterward, Yerokhin *et al.*[14,15] have presented the results of *ab initio* calculations for several H-like ions in the range of $8 \leq Z \leq 92$, considering various QED contributions to σ, as well as Bohr-Weisskopf and quadrupole corrections. They found that QED corrections, related to total σ, are in the range from -0.002% for $_8O^{7+}$ to -0.7% for $_{83}Bi^{82+}$ (being also about 1% of the relativistic part). The Bohr-Weisskopf corrections, meaning the effect induced by the spatial distribution of the nuclear magnetic moments, and the quadrupole corrections are of the same

[a)] Electronic Supplementary Information (ESI) available. See DOI: 10.1039/b000000x
[b)] Electronic mail: mail@karol-koziol.net
[c)] Electronic mail: agustin.aucar@conicet.gov.ar
[d)] Electronic mail: gaa@unne.edu.ar

order of magnitude as the QED effects for H-like ions.[14,15] In Refs. 13, 14 and 15 the first reliable results were given, but only for 1- and 2-electron atomic systems. Theoretical treatments used in both references are fully relativistic, being that of Ref. 13 based on the non-relativistic QED expansion (only the zeroth-order approximation is obtained non-relativistically). The difficulties are such that there are no actual calculations published in the literature with estimations of such effects on σ for many-electron systems.

Among different formalisms that were developed to introduce QED effects on atomic systems,[17–21] there is the polarization propagator one which was recently derived from the path integral version of quantum theory.[22] This fact gives new insights on how to include QED and correlation effects altogether, through the consideration of the effects of external perturbations on a many-body quantum system that is described within a QED-based theoretical framework. Within the polarization propagator formalism perturbative (external) effects can be described by using the knowledge of the unperturbed though correlated many-body quantum system.

Recently we published preliminary results concerning the estimation of QED effects on NMR shielding constant for He-like and Be-like atomic systems with $10 \leq Z \leq 86$.[23] In that work we presented a model by which QED corrections, obtained by Yerokhin *et al.* for H-like atoms, are scaled to those ionic systems.[14,15] Such procedure is similar to the way QED effects are usually introduced in multi-electron atoms.[24] We also estimated the Gaunt corrections to the molecular orbital energies of few diatomic molecules, *i.e.* HX (X = Br, I, At).[25]

As a next step in our research program to include QED effects on atomic and molecular properties, in this manuscript we give an estimation of QED effects on shielding of neutral and ionic atoms with $10 \leq Z \leq 86$, and diatomic halogen molecules by using an extension of our previous approach. To our knowledge there is no other estimation of QED effects on nuclear shielding of molecular systems. Our results show that QED effects may be measurable. At the moment highly accurate absolute values of NMR shieldings in some gas-phase molecules can be obtained by experiments. Their error bars may be less than the values of QED corrections for heavy-atom containing molecules.[26–29]

We also include the analysis of the physical mechanisms that are involved in both relativistic terms, ee (or paramagnetic-like) and pp (or diamagnetic-like). We shall show that the origin of the pp-like term may be understood, within the polarization propagator formalism, as due to the propagation of virtual electron-positron pairs.[6,22,30] This is shown through the analysis of the nuclear shielding of ions of the same nucleus.

In the following sections we will present two different models for including QED effects on shielding of ionic and neutral atoms, together with diatomic molecules. We shall consider relativistic contributions to the shieldings of those systems and propose a Z-dependence for QED effects on the shieldings of neutral atoms. We shall also show the pattern that QED corrections follows in all those systems.

II. THEORETICAL MODELS AND COMPUTATIONAL DETAILS

In this section we sketch few basic expressions of the underlying theoretical method used for relativistic calculations. Then we present two models for including QED effects on magnetic shieldings. The first one is the same as given previously,[23] and the second one is less accurate though useful for our purpose. Computational details are also given.

A. The NMR shieldings

Within the polarization propagator formalism, the shielding constant of nucleus K, $\sigma(K)$, is written at first consistent order of approach or random phase approximation (RPA) as[6]

$$\sigma(K) \;=\; \begin{pmatrix} \boldsymbol{b}^K & \boldsymbol{b}^{*K} \end{pmatrix} \begin{pmatrix} \boldsymbol{A} & \boldsymbol{B}^* \\ \boldsymbol{B} & \boldsymbol{A}^* \end{pmatrix}^{-1} \begin{pmatrix} \boldsymbol{b}^{*B} \\ \boldsymbol{b}^{B} \end{pmatrix} \qquad (1)$$

where K corresponds to the nuclear magnetic moment index, B is the external magnetic field, and Gaussian cgs system of units are used. There are two different terms on the rhs of Eq. (1). The first one and the last one are so-called *perturbators*, $\boldsymbol{b}$, and the matrix in the middle correspond to the *principal propagator*, $\boldsymbol{P} = \boldsymbol{M}^{-1}$, being matrices $\boldsymbol{A}$ and $\boldsymbol{B}$ written within the second quantization language as,

$$\begin{aligned} \boldsymbol{A}_{ia,jb} &= -\langle 0|[a_i^\dagger a_a, [a_b^\dagger a_j, H_0]]|0\rangle = \delta_{ab}\delta_{ij}(\varepsilon_a - \varepsilon_i) \;+\; \langle aj||ib\rangle \\ &= A_{ia,jb}(0) \;+\; A_{ia,jb}(1) \end{aligned} \qquad (2)$$

and

$$\boldsymbol{B}_{ia,jb} = \langle 0|[a_a^\dagger a_i, [a_b^\dagger a_j, H_0]]|0\rangle = -\langle ji||ab\rangle. \qquad (3)$$

Subscripts $a, b, \ldots$ refer to canonical unoccupied Dirac-Hartree-Fock (DHF) orbitals and $i, j, \ldots$ stands for canonical occupied DHF orbitals and H_0 refers to the unperturbed electronic Hamiltonian.

Eq. (1) is valid within both regimes, relativistic and NR, though the actual expressions of its three factors depends on the framework one works in. In what follows all expressions will be given within the relativistic framework.

Both perturbators are written as

$$\boldsymbol{b}_{ia}^K = \left\langle i \left| \frac{\boldsymbol{\alpha} \times \boldsymbol{r}_K}{r_K^3} \right| a \right\rangle, \quad \boldsymbol{b}_{jb}^B = \langle j| \frac{\boldsymbol{\alpha} \times \boldsymbol{r}_G}{2} |b\rangle \qquad (4)$$

where $\boldsymbol{r}_G = \boldsymbol{r} - \boldsymbol{R}_G$ being $\boldsymbol{R}_G$ the gauge origin, and $\boldsymbol{r}_K = \boldsymbol{r} - \boldsymbol{R}_K$, being $\boldsymbol{R}_K$ the position of nucleus K. They

are related with excitations from occupied to unoccupied orbitals. In the relativistic regime the set of unoccupied orbitals is splitted into two subsets, the positive and negative branch of energies. Excitations from occupied electronic states to negative (pp) and positive (ee) energy solutions are related with the pp or diamagnetic-like, σ^{pp}, and ee or paramagnetic-like, σ^{ee}, contributions to σ.[22,30]

As mentioned in Ref. 23 actual calculations are not performed using Eq. (1) but an algorithm that solves the product among the inverted matrix of the principal propagator (which is the inverse of the electronic Hessian) and one of the perturbators

$$\sigma(K) = \sum_{ia,jb} \left(\boldsymbol{b}_{ia}^{K}\ \boldsymbol{b}_{ia}^{*K}\right)\ (\boldsymbol{M}^{-1})_{ia,jb} \begin{pmatrix} \boldsymbol{b}_{jb}^{*B} \\ \boldsymbol{b}_{jb}^{B} \end{pmatrix} \tag{5}$$

$$= \sum_{ia} \left(\boldsymbol{b}_{ia}^{K}\ \boldsymbol{b}_{ia}^{*K}\right)\ \begin{pmatrix} \boldsymbol{X}_{ia}^{*B} \\ \boldsymbol{X}_{ia}^{B} \end{pmatrix} = \sum_{ia} \sigma_{ia}(K) \tag{6}$$

All the information related to the principal propagator and one of the two perturbators is contained in the matrix $\mathbf{X}$. The way it is formally derived and implemented in the four-component Dirac code is explicitly given in Ref. 31.

B. Estimating QED effects – model A

This model was first proposed in Ref. 23. We have made a consideration that leading QED corrections to both, perturbators and principal propagators are enough to estimate an order of magnitude for QED corrections to shieldings.

In the papers of Yerokhin *et al.*[14,15] the NMR shielding constants for H-like ions are calculated within Rayleigh-Schrödinger sum-over-states perturbation theory by considering virtual excitations from ground $1s_{1/2}$ state to excited $ns_{1/2}$ electronic Dirac states. This model is based on earlier works of Moore[32] and Pyper[33]. In Yerokhin *et al.* work the QED correction to the shielding constant is calculated as a sum of various vacuum polarization (VP) and self energy (SE) contributions and expressed in terms of the function $D(Z\alpha)$ as

$$\Delta\sigma^{QED} = \Delta\sigma^{SE} + \Delta\sigma^{VP} \tag{7}$$

$$\Delta\sigma^{SE} = \alpha^2(Z\alpha)^3 D_{SE}(Z\alpha) \tag{8}$$

$$\Delta\sigma^{VP} = \alpha^2(Z\alpha)^3 D_{VP}(Z\alpha) \tag{9}$$

where $\Delta\sigma^{VP}$ collects VP influence on both electronic orbital properties (perturbed-orbital contribution, $\Delta\sigma^{VP,po}$) and hyperfine interaction ($\Delta\sigma^{VP,mag}$), *i.e.*

$$\begin{aligned}\Delta\sigma^{VP} &= \Delta\sigma^{VP,po} + \Delta\sigma^{VP,mag} \\ &= \alpha^2(Z\alpha)^3 D_{VP,po}(Z\alpha) + \alpha^2(Z\alpha)^3 D_{VP,mag}(Z\alpha)\end{aligned} \tag{10}$$

Then the ratio

$$R_D = \frac{D_{VP,po}(Z\alpha)}{D_{VP}(Z\alpha) + D_{SE}(Z\alpha)} = \frac{\Delta\sigma^{VP,po}}{\Delta\sigma^{QED}} \tag{11}$$

is a relative contribution of perturbed-orbital VP contribution to total QED effect.

In our study we assume that the pattern of SE to VP effects ratio, expressed by $D_{SE}(Z\alpha)$, $D_{VP}(Z\alpha)$, and $D_{VP,po}(Z\alpha)$ coefficients, is similar for H-like and many-electron atomic systems. That happens in the case of orbital energies – compare, *e.g.*, Ref. 34 and supplement of Ref. 35. The VP influence on principal propagator is equivalent to adding VP energy correction to appropriate orbitals energies. The perturbed-orbital VP influence on perturbators can be reproduced in many-electron atoms by comparing calculations with and without Uehling potential included in self-consistent field (SCF) process. Let us make the following ratios

$$\begin{aligned}C_B(\tfrac{DCBV}{DCB}) &= \frac{(n_1\kappa_1 m_1 \boldsymbol{\alpha}\times\boldsymbol{r} n_2\kappa_2 m_2)_{DCBV}}{(n_1\kappa_1 m_1 \boldsymbol{\alpha}\times\boldsymbol{r} n_2\kappa_2 m_2)_{DCB}} \\ &= \frac{\left(R^{(1)}(n_1\kappa_1 n_2\kappa_2)\right)_{DCBV}}{\left(R^{(1)}(n_1\kappa_1 n_2\kappa_2)\right)_{DCB}}\end{aligned} \tag{12}$$

and

$$\begin{aligned}C_K(\tfrac{DCBV}{DCB}) &= \frac{\left(n_1\kappa_1 m_1 \frac{\boldsymbol{\alpha}\times\boldsymbol{r}}{r^3} n_2\kappa_2 m_2\right)_{DCBV}}{\left(n_1\kappa_1 m_1 \frac{\boldsymbol{\alpha}\times\boldsymbol{r}}{r^3} n_2\kappa_2 m_2\right)_{DCB}} \\ &= \frac{\left(R^{(-2)}(n_1\kappa_1 n_2\kappa_2)\right)_{DCBV}}{\left(R^{(-2)}(n_1\kappa_1 n_2\kappa_2)\right)_{DCB}}\end{aligned} \tag{13}$$

being both indices DCB and $DCBV$ mean wavefunctions calculated in a self-consistent manner by using Dirac–Coulomb–Breit Hamiltonian without and with adding the Uehling potential, respectively. Besides $R^{(n)}$ are the radial integrals defined as

$$R^{(n)}(n_1\kappa_1 n_2\kappa_2) = \int_0^\infty r^n (P_{n_1\kappa_1} Q_{n_2\kappa_2} + Q_{n_1\kappa_1} P_{n_2\kappa_2}) dr \tag{14}$$

being $P_{n\kappa}$ and $Q_{n\kappa}$ the radial parts of the one-electron wavefunction (Dirac bispinor). The $C_K(\frac{DCBV}{DCB})$ and $C_B(\frac{DCBV}{DCB})$ factors count the VP effects on both perturbators of Eq. (4). It is worth to mention that $C_K(\frac{DCBV}{DCB})$ factors are larger than $C_B(\frac{DCBV}{DCB})$ factors or, in other words, the expectation value of $\frac{\boldsymbol{\alpha}\times\boldsymbol{r}}{r^3}$ operator is more influenced by VP than the one for $\boldsymbol{\alpha}\times\boldsymbol{r}$ operator. Then the coefficient $C^{VP/DC}$ expressed as

$$C^{VP/DC} = C_K(\tfrac{DCBV}{DCB}) C_B(\tfrac{DCBV}{DCB}) - 1 \tag{15}$$

accounts for perturbed-orbital VP influence on both perturbators. Index DC means the Dirac–Coulomb–Breit level of theory, without QED corrections. We should also mention that factors $C^{VP/DC}$ in each of the following group of excitations: $ns - n's$, $np_{1/2} - n'p_{1/2}$,

$np_{3/2} - n'p_{3/2}$, etc. depends weakly on n'. So, it is justified to use only one $C^{VP/DC}$ factor for each of those group of orbitals.

Next, let us use the following auxiliary symbols:

$$m_{ia}^{K} = \frac{1}{2c^2}\langle i|(c\boldsymbol{\alpha}\times\boldsymbol{r}_G)|a\rangle\langle a|\frac{(c\boldsymbol{\alpha}\times\boldsymbol{r}_K)}{r_K^3}|i\rangle$$

$\Delta\varepsilon_{ia} = \varepsilon_i^{DC} - \varepsilon_a^{DC}$, $\Delta\varepsilon_{ia}^{VP} = \Delta\varepsilon_i^{VP} - \Delta\varepsilon_a^{VP}$ for simplification. Then using Eq. (1)

$$\begin{aligned}\sigma_{ia}^{DC+VP,po} &= \frac{m_{ia}^{DCV}}{\Delta\varepsilon_{ia}+\Delta\varepsilon_{ia}^{VP}} = \frac{m_{ia}^{DC}\left(1+C_{ia}^{VP/DC}\right)}{\Delta\varepsilon_{ia}+\Delta\varepsilon_{ia}^{VP}} \\ &= \sigma_{ia}^{DC} + \Delta\sigma_{ia}^{VP,po} = \frac{m_{ia}^{DC}}{\Delta\varepsilon_{ia}} + \Delta\sigma_{ia}^{VP,po}\end{aligned} \tag{16}$$

After short derivations:

$$\Delta\sigma_{ia}^{VP,po} = \frac{m_{ia}^{DC}\left(C_{ia}^{VP/DC} - \frac{\Delta\varepsilon_{ia}^{VP}}{\Delta\varepsilon_{ia}}\right)}{\Delta\varepsilon_{ia}+\Delta\varepsilon_{ia}^{VP}} \tag{17}$$

Next, we can write:

$$\begin{aligned}\sigma_{ia}^{DC+QED} &= \sigma_{ia}^{DC} + \Delta\sigma_{ia}^{QED} = \sigma_{ia}^{DC} + \sigma_{ia}^{DC}C_{ia}^{QED/DC} \\ &= \sigma_{ia}^{DC} + \Delta\sigma_{ia}^{VP,po}\frac{\Delta\sigma_{ia}^{QED}}{\Delta\sigma_{ia}^{VP,po}} \\ &= \frac{m_{ia}^{DC}}{\Delta\varepsilon_{ia}} + \Delta\sigma_{ia}^{VP,po}R_D^{-1}\end{aligned} \tag{18}$$

where the scaling coefficients $C_{ia}^{QED/DC}$ is introduced. Finally, linking Eq. (17) and Eq. (18) we obtain the $C^{QED/DC}$ coefficient in the form

$$C_{ia}^{QED/DC} = \left(\frac{C_{ia}^{VP/DC} - \Delta_{ia}^{VP}}{1+\Delta_{ia}^{VP}}\right)R_D^{-1} \tag{19}$$

when a is a positive-energy unoccupied state. If a is one of the negative-energy unoccupied states, $C_{ia}^{QED/DC} = 0$. For simplicity we used the factor $\Delta_{ia}^{VP} = \Delta\varepsilon_{ia}^{VP}/\Delta\varepsilon_{ia}$.

Then we are able to rewrite Eq. (6) to include leading-order QED effects within polarization propagator formalism at zeroth- and first-order level of approach:

$$\begin{aligned}\sigma^{DC+QED}(K) &= \sum_{\substack{i=\text{inner s-type},\\ a=\text{unoccupied s-type}}} \sigma_{ia}^{DC}(K)\left(1+C_{ia}^{QED/DC}\right) \\ &+ \sum_{\substack{i=\text{inner s-type},\\ a\neq\text{unoccupied s-type}}} \sigma_{ia}^{DC}(K) \\ &+ \sum_{\substack{i\neq\text{inner s-type},\\ a}} \sigma_{ia}^{DC}(K)\end{aligned} \tag{20}$$

In this equation the amplitudes for excitations between atomic or molecular orbitals are scaled by coefficients $C_{ia}^{QED/DC}$.

The more general approach[30] considers excitations from occupied electronic states to both positive- (electronic) and negative-energy (positronic) unoccupied Dirac states, resulting in the ee and pp contributions, respectively. In order to ensure the compatibility between the approaches of Yerokhin *et al.* and ours, we implemented QED corrections only to the ee term of shielding. Coefficients D_{SE}, D_{VP}, and $D_{VP,po}$ have been calculated for H-like systems, in such a way that the use of $C^{QED/DC}$ factor is justified only for $ns - n's$ excitations. Assuming that the pattern of SE to VP effects ratio is similar for each ns subshell, as happens in the case of orbital energies (see supplement of Ref. 35), we extended our model for excitations from ns subshells with $n > 1$.

C. Estimating QED effects – model B

There are few approaches to estimate the influence of QED effects on orbital energies, in many-electron atoms.[24,35] The original idea of Bethe[36] linked the QED contribution to ns orbital energies with the electron density at the site of the nucleus. We test this simple model in the case of QED contributions to shielding constants:

$$\Delta\sigma^{QED} = \Delta\sigma_{Hyd}^{QED}\sum_n \frac{\rho(0)_{ns}}{\rho(0)_{ns,Hyd}}\frac{\sum_a \sigma_{ns,a}}{\sum_a \sigma_{1s,a}^{Hyd}} \tag{21}$$

where $\Delta\sigma_{Hyd}^{QED}$ is calculated by Eq. (7), according to Ref. 15, and σ_{ia} was defined in Eq. (5) (a is an unoccupied electronic state).

D. QED effects on the shielding constants of nuclei in molecules

For the calculation of nuclear shieldings in molecules within polarization propagators, the occupied and vacant atomic orbitals, AOs, i, j and a, b, respectively, are replaced by their molecular orbitals, MOs, counterparts.

In order to estimate their QED effects we assume that

- They will modify the contributions due to perturbators but not much the matrix elements of the principal propagator. Then we can use the same criterium for including QED effects in molecules as used for atoms; meaning, by applying coefficients $C^{QED/DC}$
- They are mostly due to excitations arising from the occupied MOs that are built from s-type GTO. These MOs are σ bonding and antibonding orbitals. Furthermore, the inner occupied MOs are close in energy to the inner AOs of the atom to whom that nucleus belongs. Then we can use $C^{QED/DC}$ for

including QED effects due to the innermost s-type MOs.

In order to be more clear about the way we included the ee contributions to the shielding on molecules, it is better to rearrange the summation of the rhs of Eq. (20) into two parts. The one that include QED effects on top of contributions of the $ns - n's$ MOs excitations and another one that only consider relativistic contributions. This scheme of calculation will be given more explicitly in the next section.

E. Computational details

1. MCDF method

The calculation of $C(\frac{DCBV}{DCB})$ coefficients, the radial integrals defined in Eq. (14), and QED contributions to the orbital energies were performed by means of MCDFGME code release 2005[37,38]. This four-component code is based on the well-established Multiconfigurational Dirac–Fock (MCDF) approach.

The methodology of MCDF calculations performed in the present studies is similar to the one published earlier, in several papers (see, e.g., 39,40). The effective Dirac–Coulomb–Breit Hamiltonian for an N-electron system is expressed by

$$\hat{H} = \sum_{i=1}^{N} \hat{h}_D(i) + \sum_{j>i=1}^{N} V_{ij} \tag{22}$$

where $\hat{h}_D(i)$ is the Dirac one-particle operator for i-th electron and the terms $\hat{V}_{ij}$ account for the effective electron-electron interactions.

An atomic state function (ASF) with the total angular momentum J, its z-projection M, and parity p is assumed in the form

$$\Psi_s(JM^p) = \sum_m c_m(s)\Phi(\gamma_m JM^p) \tag{23}$$

where $\Phi(\gamma_m JM^p)$ are configuration state functions (CSF), $c_m(s)$ are the configuration mixing coefficients for state s, γ_m represents all information required to uniquely define a certain CSF. The CSF is a Slater determinant of Dirac 4-component bispinors:

$$\Phi(\gamma_m JM^p) = \sum_i d_i \begin{vmatrix} \psi_1(1) & \cdots & \psi_1(N) \\ \vdots & \ddots & \vdots \\ \psi_N(1) & \cdots & \psi_N(N) \end{vmatrix} \tag{24}$$

where the ψ_i is the one-electron wavefunctions and the d_i coefficients are determined by requiring that the CSF is an eigenstate of $\hat{J}^2$ and $\hat{J}_z$. The one-electron wavefunction is defined as

$$\psi_{n,\kappa,j} = \frac{1}{r}\begin{pmatrix} P_{n,\kappa}(r)\cdot\Omega^{m_j}_{\kappa,j}(\theta,\phi) \\ iQ_{n,\kappa}(r)\cdot\Omega^{m_j}_{-\kappa,j}(\theta,\phi) \end{pmatrix} \tag{25}$$

where $\Omega^{m_j}_{\kappa,j}(\theta,\phi)$ is a angular 2-component spinor and $P_{n,\kappa}(r)$ and $Q_{n,\kappa}(r)$ are large and small radial part of the wavefunction, respectively.

The electron-electron interaction term is a sum of the Coulomb interaction $\hat{V}^C_{ij}$ operator and the transverse Breit $\hat{V}^B_{ij}$ operator:[41]

$$\hat{V}_{ij} = \hat{V}^C_{ij} + \hat{V}^B_{ij} \tag{26}$$

where the Coulomb interaction operator is $\hat{V}^C_{ij} = 1/r_{ij}$, and the Breit operator

$$\hat{V}^B_{ij} = -\boldsymbol{\alpha}_i\cdot\boldsymbol{\alpha}_j\frac{e^{i\omega_{ij}r_{ij}}}{r_{ij}} - (\boldsymbol{\alpha}_i\cdot\boldsymbol{\nabla}_i)(\boldsymbol{\alpha}_j\cdot\boldsymbol{\nabla}_j)\frac{e^{i\omega_{ij}r_{ij}}-1}{\omega^2_{ij}r_{ij}} \tag{27}$$

where $\omega_{ij} = (\varepsilon_i - \varepsilon_j)/c$ is the frequency of one virtual photon exchanged (ε_i and ε_j are orbital energies of interacting electrons).

The Uehling potential,[42] being the first term of vacuum polarization contribution of order $\alpha(Z\alpha)$, in the case of finite nuclear size and spherical symmetric nuclear charge distribution $\rho(\vec{r})$ can be expressed as:[43]

$$U(\vec{r}) = -\frac{2}{3}\frac{Z\alpha^2\hbar^2}{mr}\int_0^\infty d^3r'\, r'\rho(r') \times\left[K_0\left(\frac{2mc}{\hbar}|r-r'|\right) - K_0\left(\frac{2mc}{\hbar}|r+r'|\right)\right] \tag{28}$$

where the function $K_0(x)$ is defined as:

$$K_0(x) = \int_1^\infty dt\, e^{-xt}\left(\frac{1}{t^3}+\frac{1}{2t^5}\right)\sqrt{t^2-1} \tag{29}$$

The Uehling potential in atomic self-consistent field calculations that can be treated perturbatively or in self-consistent way.[35] In the last case, the regular Hartree–Fock equations (where $\hat{F}$ is a Fock operator according to Dirac–Coulomb–Breit Hamiltonian, ψ_k is an one-electron wavefunction (orbital), and ε_k is an orbital energy.)

$$\hat{F}\psi_k = \varepsilon_k\psi_k \tag{30}$$

are transformed into new Hartree–Fock equations

$$(\hat{F}+U)\psi'_k = \varepsilon'_k\psi'_k \tag{31}$$

where Uehling potential, U, is added to eigenvalue equation, and ψ'_k and ε'_k are modified orbital and orbital energy, respectively.

The radial integrals specified in Eq. 14 have been calculated by using intrinsic function of MCDFGME code.

2. NMR shielding constant calculations

The calculations of NMR shielding constants were performed by means of the DIRAC code release 2017.[44] The Gaussian nuclear charge distribution was used.[45] We used for Ne, Ar,[46] Br, Kr, I, Xe, At, and Rn[47] the dyall.acv4z basis set and for Zn,[48] Cd,[49] and Hg,[50] the dyall.cv4z basis set. NR values of σ were obtained performing pseudo-nonrelativistic calculations by assuming the speed of light as $c = 100c_0$ (being $c_0 = 137.0359998$ a.u.).

Because the DIRAC code has issues related to open-shell systems, the $\sum_a \sigma^{Hyd}_{1s,a}$ values in Eq. (21) are actually extracted from calculations performed for point-like H-like systems[33] and corrected by finite nuclear size (FNS) effect by using proportionally values of FNS (calculated by DIRAC code) for He-like ions.

Four-component calculations of shieldings are based on the Dirac–Coulomb and Dirac–Coulomb–Gaunt Hamiltonians. Due to actual implementations in the DIRAC code, Gaunt contributions to the shieldings are partially included in both kind of terms of Eq. (5). They are included in the matrix elements of the principal propagator through the orbital energies (occupied and virtual). For perturbators they are included through the matrix elements of the Fock matrix that is one-index transformed. There are no Gaunt contributions included in the two-electron elements of the principal propagator.[31] Furthermore, we should highlight that the Breit electron-electron interactions are replaced by Gaunt integrals, *i.e.* the retardation terms are neglected. We assume that Gaunt interactions provide a useful approximation to the Breit interactions; they were found to be an order of magnitude larger than the retardation contributions.[25]

Linear response calculations were performed within the relativistic polarization propagator approach at the random phase level of approach (RPA). Two-electron integrals containing only small component basis functions, the (SS|SS) integrals, were included in all calculations.

In all cases, the uncontracted Gaussian basis sets were used with the common gauge-origin (CGO) approach. The small component basis sets for relativistic calculations were generated by applying the unrestricted kinetic balance prescription (UKB).

In the DIRAC code MOs are expanded in a gaussian basis set in such a way that s-type, p-type, etc gaussian functions are used. Then Large and Small s-type components are expanded in a set of s-type gaussian functions so that we can use the scaled $C^{QED/DC}_{1s,ns}$, $C^{QED/DC}_{2s,ns}$, ... coefficients for including QED corrections arising from the innermost s-type MOs. For the molecules analyzed here, we found that the first term on the rhs of Eq. (20) dominates over the second term, i.e. the contribution of excitations starting from inner s-type MO that end up on s-type unoccupied MOs is very high (larger than 90 %):

$$\frac{\sum\limits_{\substack{i=\text{inner s-type},\\ a=\text{unoccupied s-type}}} \sigma^{DC}_{i,a}(K)}{\sum\limits_{\substack{i=\text{inner s-type},\\ a}} \sigma^{DC}_{i,a}(K)} > 0.9 \tag{32}$$

Then, in practice, we calculate σ^{DC+QED} by using simplified form of Eq. (20):

$$\begin{aligned}\sigma^{DC+QED}(K) &= \sum_{\substack{i=\text{inner s-type},\\ a}} \sigma^{DC+QED}_{ia}(K) \\ &+ \sum_{\substack{i\neq\text{inner s-type},\\ a}} \sigma^{DC}_{ia}(K)\end{aligned} \tag{33}$$

with the error of calculations about 5%. We used the special output of DIRAC code to make such kind of analysis. We show how to actually do it in Supplementary Information for I_2 molecule.

The gauge origin of the external magnetic potential was placed at the molecular center of mass in all the NMR shielding calculations. Furthermore, when necessary the shieldings were calculated for the anions rather the neutral atoms in order to have closed-shell systems.

Experimental bond distances were extracted from Ref. 51 for HBr, HI, Br_2 and I_2. For HAt and At_2, optimized distances were employed, and calculated at DHF level of approach. The internuclear distances are: 1.4145 Å (HBr), 1.6090 Å (HI), 2.2811 Å (Br_2), 2.6663 Å (I_2), 1.7117 Å (HAt) and 2.9627 Å (At_2).

III. RESULTS AND DISCUSSIONS

We shall show first results at RPA level of approach of four-component calculations of shielding for neutral atoms and ions separated in paramagnetic-like and diamagnetic-like as is usual within the NR regime. This analysis will show the origin of novel behaviors that appear for the first time in the present work. Relativistic effects are then analyzed and compared with NR contributions. Gaunt contributions (which are partially included as mentioned in the previous Section) to the relativistic effects are also given. The pattern of QED contributions to the atomic and diatomic molecular systems are then given, together with the analysis of which excitations are more involved. In our previous article[23] we have included only few of total excitations. We shall end up with the analysis of the dependence of QED effects on the shielding of atoms and molecules, and compare them with relativistic and NR effects.

TABLE I. NMR shielding constants (without QED contributions, but employing the Dirac–Coulomb–Gaunt Hamiltonian) for Ne, Ar, Zn, Kr, and Cd neutral atoms, and their ions. σ^t means total shielding and σ^{pp} and σ^{ee} mean diamagnetic-like and paramagnetic-like terms, respectively. σ^{Lamb} stand for numbers calculated by the Lamb expression. n_{el} is the number of electrons in the ion.

Z	n_{el}	σ^t (ppm)	σ^{pp} (ppm)	σ^{ee} (ppm)	σ^{Lamb} (ppm)
10	2	348.8549	338.1047	10.7501	342.3263
	4	421.3373	409.6369	11.7004	400.4438
	10	557.1123	545.1253	11.9870	553.3895
18	2	656.4766	598.0950	58.3816	628.4583
	4	803.1269	738.6204	64.5065	755.8693
	10	1156.6681	1090.1447	66.5234	1124.4790
	12	1195.9558	1128.6501	67.3058	1158.8409
	18	1273.1343	1205.4665	67.6679	1245.6581
30	2	1196.1820	924.0793	272.1027	1073.2668
	4	1465.2827	1162.2390	303.0437	1309.4299
	10	2149.9452	1833.8730	316.0722	1998.8822
	12	2240.5185	1918.4602	322.0582	2072.9265
	18	2466.5450	2141.9852	324.5598	2277.7234
	30	2708.5417	2380.5594	327.9823	2564.3647
36	2	1522.3339	1055.0074	467.3265	1305.3292
	4	1861.1178	1339.3208	521.7970	1598.4356
	10	2716.8037	2171.1266	545.6771	2450.7825
	12	2835.1619	2278.0196	557.1423	2547.4234
	18	3135.6392	2573.5528	562.0864	2819.8878
	30	3520.6708	2952.8542	567.8166	3252.5333
	36	3584.5022	3014.7361	569.7661	3324.2802
48	2	2358.6725	1247.4817	1111.1908	1797.8509
	4	2865.7675	1619.5662	1246.2014	2213.7973
	10	4082.0652	2770.4307	1311.6345	3403.7627
	12	4263.8099	2920.9406	1342.8693	3550.2714
	18	4718.6823	3360.6799	1358.0024	3966.4257
	30	5382.5622	4006.6724	1375.8898	4669.1920
	36	5537.2706	4157.2339	1380.0368	4817.9820
	48	5712.6538	4328.3407	1384.3131	5020.0663

TABLE II. Like Table I, but for Xe, Hg, and Rn neutral atoms, and their ions.

Z	n_{el}	σ^t (ppm)	σ^{pp} (ppm)	σ^{ee} (ppm)	σ^{Lamb} (ppm)
54	2	2906.9916	1306.3837	1600.6080	2062.9539
	4	3519.7615	1720.6408	1799.1206	2546.1461
	10	4928.7650	3032.2250	1896.5400	3912.4090
	12	5148.0911	3204.2655	1943.8256	4085.7798
	18	5684.1065	3716.6786	1967.4279	4576.4484
	30	6489.9526	4494.3249	1995.6277	5412.6441
	36	6689.2415	4686.5192	2002.7223	5602.9513
	48	6951.7593	4942.6570	2009.1024	5894.0158
	54	7012.5684	4993.4026	2019.1658	5953.2268
80	2	7334.7492	1216.0226	6118.7266	3461.2741
	4	8787.6229	1816.5725	6971.0503	4314.2259
	10	11 235.8003	3828.0459	7407.7544	6541.5774
	12	11 722.6113	4097.2880	7625.3233	6855.0454
	18	12 675.3055	4931.0022	7744.3034	7700.9773
	30	14 153.6585	6272.4815	7881.1770	9123.3277
	36	14 569.7331	6646.0210	7923.7120	9479.9783
	46	15 122.0610	7174.3572	7947.7038	10 005.0399
	60	15 695.6976	7718.4575	7977.2401	10 465.4841
	80	16 043.8386	8038.3147	8005.5239	10 998.2549
86	2	9247.5992	1108.1436	8139.4556	3875.8111
	4	11 077.3338	1761.2554	9316.0784	4842.9054
	10	13 854.4739	3944.0385	9910.4354	7302.8837
	12	14 452.8551	4239.2752	10 213.5799	7657.1837
	18	15 530.6210	5150.9483	10 379.6727	8596.1049
	30	17 188.1006	6622.3589	10 565.7417	10 160.0066
	36	17 666.7068	7039.1203	10 627.5865	10 562.4473
	46	18 294.0091	7634.4209	10 659.5882	11 154.7362
	60	18 972.1586	8274.3071	10 697.8515	11 700.4071
	80	19 441.4233	8693.8250	10 747.5983	12 356.5946
	86	19 660.0728	8740.4598	10 919.6130	12 411.9911

A. Relativistic and non-relativistic contributions

We should first mention that all relativistic calculations were performed using the Dirac–Coulomb–Gaunt Hamiltonian. Tables I and II collect calculated NMR shielding constants (without QED contributions) for closed-shell $_{10}$Ne, $_{18}$Ar, $_{30}$Zn, $_{36}$Kr, $_{48}$Cd, $_{54}$Xe, $_{80}$Hg, and $_{86}$Rn neutral atoms, and their selected closed-shell ions. We included in them both contributions, σ^{pp} and σ^{ee}, which are equivalent to diamagnetic-like and paramagnetic-like terms well defined within the NR framework.[30] For low- and medium-Z atoms, the diamagnetic-like term contributes more than the paramagnetic-like one, but for high-Z atoms this behavior is reversed.

One can see that the diamagnetic-like contributions strongly depend on the actual number of electrons that are bonded to the ionized atoms (n_{el}), but the paramagnetic dependence on them is much smaller. These differences show that they arises from two different physical origins.

The major contributions to σ^{ee} arises from electron-electron excitations that start from the $1s$ shell, even for neutral atoms. The next important part of those excitations start from the $2s$ shell (and then appears those starting from higher ns shell for high-Z atoms). For example, for Be-like ($n_{el} = 4$) Ne the e-e excitations from the $1s$ shell contribute 82.42% and excitations from the $2s$ shell contribute 17.58%. For Be-like Rn these numbers are 65.29% and 34.71% respectively. For neutral Ne ($n_{el} = 10$) the e-e excitations from the $1s$ shell contribute 82.57% and excitations from the $2s$ shell contribute 13.69%. For neutral Rn ($n_{el} = 86$) these numbers are 52.35% and 21.16% respectively. One can see that with increasing Z the percentual contributions from 2s shell excitations increase and those from the $1s$ shell decrease.

The percentage of contributions to the relativistic value of σ^{ee} of He-, Be-, Ne-like and neutral Rn atoms are shown in Fig. 1. For He-like Rn the excitation $1s \to 2s$ ($1s \to 3s$) contributes $\approx 25.4\%$ ($\approx 5.6\%$). The other important contributions arises from excitations to the

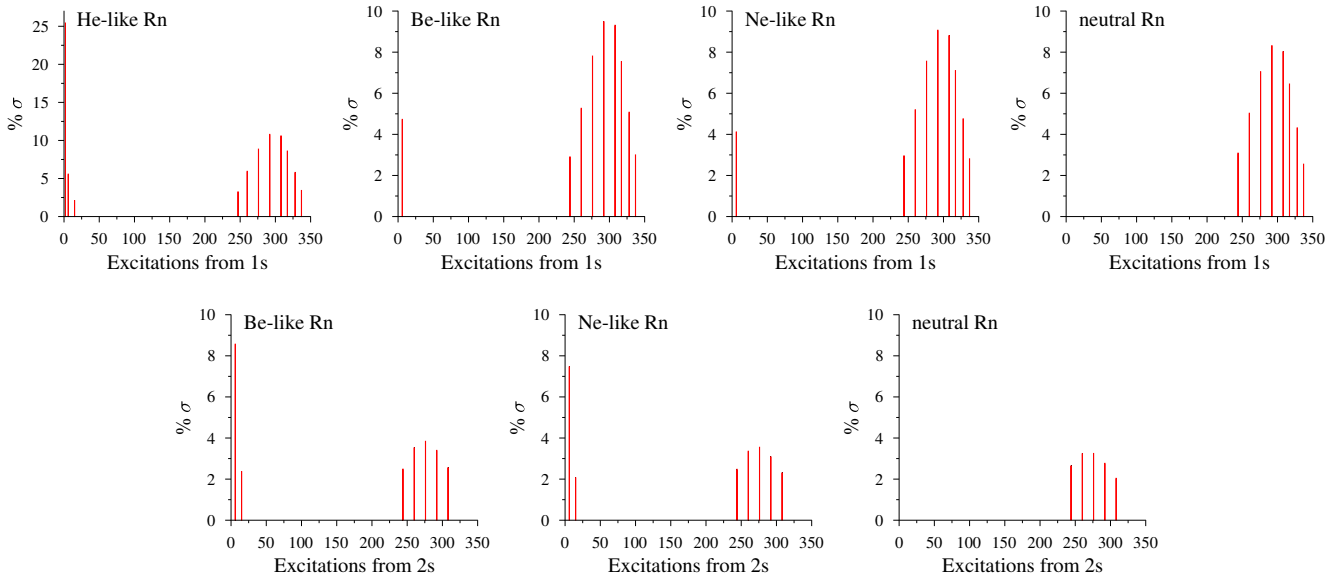

FIG. 1. Pattern of percentage contributions of leading e-e excitations starting from $1s$ and $2s$ orbitals for He-, Be-, Ne-like, and neutral Rn. Excitations to unoccupied, bounded and unbounded AOs are displayed. The pattern for neutral Rn contains only excitations to unbounded AOs.

high-excited ns orbitals (near continuous orbitals). For Be-like Rn the excitation $1s \to 2s$ are not allowed, and the excitation $1s \to 3s$ ($2s \to 3s$) contributes $\approx 4.7\%$ ($\approx 8.5\%$). In this case the major part of σ^{ee} contributions are originated from $1s \to ns$ and $2s \to ns$ excitations. There is a similar behavior for Ne-like Rn. In the case of neutral Rn, excitations between inner s shells are not allowed and so, contributions are due to $1s \to ns$ and $2s \to ns$ excitations.

We want to highlight here another interesting behavior of the largest contributions to σ^{ee}. The contributions of each of the total $1s \to ns$ and $2s \to ns$ excitations does not depend much on n_{el} for a given Z. Still each one of them contribute little less when the other excitations come into play. For example, the contribution from total $1s \to ns$ excitations is almost the same until the $2s \to ns$ excitations start to contribute. In such a case the total contribution of excitations arising from $1s$ orbitals diminish a little bit its value. The same happens to both, $1s \to ns$ and $2s \to ns$ excitations when excitations arising from $3s$ orbitals start to contribute.

All this explains the behavior of σ^{ee} in the whole family of ions studied in this work, which clearly is due to a relativistic effect that affect in the same manner each kind of s-type excitation mentioned above for a given Z. They do not depend on the occupation number n_{el} for the whole family of ions of a given atom. We stress that σ^{ee} is zero within the NR framework.

What about the pattern of electronic contributions to σ^{pp}? It is different from its σ^{ee} counterpart. Each subshell contributes to the excitations to the negative-energy part of the spectra, and all inner and middle shells do it with a significant value (as opposite to σ^{ee} part, where $1s$ and $2s$ subshells contribute together 75–90% to σ^{ee}). In order to be more explicit let us analyze the way σ^{pp} is built for the neutral Rn. Excitations that start in $1s$ and $2s$ AOs contribute with $\approx 12.68\%$ and 7.27%, respectively, of the total value of the shielding (*i.e.* 6.34% and 3.63% per each electronic occupation of both ns AOs, respectively). The $2p$ AOs contribute with $\approx 26.85\%$ (4.47% per electron), and the absolute value of those contributions are almost independent of whether one consider the neutral or the ionized Rn, meaning that it depends only on Z. Then, all other subshells will contribute with values that are almost the same for a given nucleus. This behavior explains why σ^{pp} grows continuously when the highly ionized atom is becoming less ionized.

From this previous analysis, and given that within our formalism σ^{pp} can be understood as due to the propagation of virtual electron-positron pairs, that involve negative-energy electronic orbitals together with positive-energy electronic orbitals, we are able to state that σ^{pp} "strongly depends" on the occupation number of electrons in each subshell, and the value of Z.

In the work of Lamb[52] there was pointed out that the diamagnetic contribution to the non-relativistic shielding is connected to the ground-state expectation value of the electrostatic potential. This was further reported in Helgaker *et al.*[53] paper, in which the simple formula for the shielding of spherically symmetrical closed-shell atoms with the gauge origin in nuclear position of the atom, was written and called Lamb expression:

$$\sigma = \frac{\alpha^2}{3}\langle 0|\frac{1}{r}|0\rangle \tag{34}$$

Even though in those previously mentioned papers it was not explictly written, on the ground of our new under-

TABLE III. Non-relativistic results for NMR shielding constants for Ne, Ar, Zn, Kr, and Cd neutral atoms, and their ions. σ^{R-NR} means the relativistic shift, *i.e.* $\sigma^{R-NR} = \sigma^{t} - \sigma^{t,NR}$. Gaunt contribution to the σ^{t} is also elucidated (Gaunt contribution is included in σ^{R-NR} but given in separate column for its further analysis).

Z	n_{el}	$\sigma^{t,NR}$ (ppm)	σ^{R-NR} (ppm)	σ^{R-NR}/σ^{t} (%)	σ^{Gaunt} (ppm)
10	2	343.9151	4.9398	1.4160	−0.1110
	4	415.8421	5.4952	1.3042	−0.1316
	10	551.1607	5.9516	1.0683	−0.1959
18	2	627.9233	28.5533	4.3495	−0.3604
	4	770.8770	32.2499	4.0155	−0.4337
	10	1121.8639	34.8042	3.0090	−0.6334
	12	1160.5729	35.3829	2.9585	−0.6678
	18	1237.2350	35.8993	2.8198	−0.7044
30	2	1053.9361	142.2459	11.8917	−0.8934
	4	1303.3988	161.8839	11.0480	−1.0978
	10	1974.2344	175.7108	8.1728	−1.7789
	12	2060.5827	179.9358	8.0310	−1.8866
	18	2283.1862	183.3588	7.4338	−2.0101
	30	2521.6519	186.8898	6.9000	−2.4096
36	2	1266.9408	255.3931	16.7764	−1.2164
	4	1569.6561	291.4617	15.6606	−1.5145
	10	2400.2900	316.5137	11.6502	−2.5746
	12	2510.3405	324.8214	11.4569	−2.7349
	18	2804.2597	331.3795	10.5682	−2.9541
	30	3183.4441	337.2267	9.5785	−3.4312
	36	3244.8743	339.6279	9.4749	−3.5179
48	2	1692.9455	665.7270	28.2246	−1.8181
	4	2102.1646	763.6029	26.6457	−2.3674
	10	3252.3564	829.7088	20.3257	−4.5276
	12	3409.7727	854.0372	20.0299	−4.8316
	18	3845.9554	872.7269	18.4951	−5.3769
	30	4492.7914	889.7708	16.5306	−6.3281
	36	4641.9163	895.3543	16.1696	−6.3789
	48	4813.0728	899.5810	15.7472	−6.8480

standings one may realize that the shielding for the whole atom is a sum of shielding contributions from particular shells. This approach may allows us to simply analyze the variation of σ with occupation of particular shells, on NR level of theory. The shielding numbers calculated by using Eq. (34) and expectation values of $1/r$ from MCDF-calculated orbitals are presented also in Tables I and II, marked as σ^{Lamb}. The numbers calculated by Lamb expression agree well, within ten percent, with pp results for shielding constants of atoms calculated by DIRAC code with $Z \leq 30$. For higher-Z atoms, the relativistic effects become important and so the difference between both kind of calculations become higher. For neutral atoms that difference is much smaller than for ionic atoms. In the case of neutral Hg the difference is close to 25% but for He-like Hg such a difference is as high as three times.

Tables III and IV collect NR results for NMR shielding constants of selected atoms and their ions. It can be seen that the paramagnetic-like term goes to zero within the

TABLE IV. Like Table III, but for Xe, Hg, and Rn neutral atoms, and their ions.

Z	n_{el}	$\sigma^{t,NR}$ (ppm)	σ^{R-NR} (ppm)	σ^{R-NR}/σ^{t} (%)	σ^{Gaunt} (ppm)
54	2	1905.9422	1001.0494	34.4359	−1.9922
	4	2368.4125	1151.3490	32.7110	−2.7048
	10	3678.3718	1250.3932	25.3693	−5.6492
	12	3859.4636	1288.6275	25.0312	−6.0481
	18	4366.7104	1317.3961	23.1768	−6.8464
	30	5146.0275	1343.9251	20.7078	−8.1215
	36	5335.9689	1353.2726	20.2306	−8.2457
	48	5591.8795	1359.8798	19.5617	−8.7942
	54	5642.0615	1370.5069	19.5436	−9.0639
80	2	2828.8500	4505.8992	61.4322	1.6319
	4	3522.0704	5265.5525	59.9201	−0.4348
	10	5524.3437	5711.4566	50.8327	−9.7077
	12	5808.0173	5914.5940	50.4546	−10.8804
	18	6623.0491	6052.2564	47.7484	−14.1050
	30	7974.2459	6179.4126	43.6595	−17.7444
	36	8338.5148	6231.2183	42.7682	−18.6334
	46	8866.2448	6255.8162	41.3688	−20.1192
	60	9414.2095	6281.4881	40.0204	−21.0645
	80	9729.8925	6313.9461	39.3543	−22.3831
86	2	3041.7961	6205.8031	67.1072	5.0326
	4	3788.2603	7289.0735	65.8017	2.2874
	10	5950.2979	7904.1760	57.0514	−9.5504
	12	6257.6240	8195.2311	56.7032	−11.1096
	18	7143.6821	8386.9389	54.0026	−15.4192
	30	8626.6467	8561.4539	49.8104	−19.9342
	36	9030.9652	8635.7416	48.8814	−21.2242
	46	9625.7345	8668.2746	47.3831	−23.1337
	60	10 270.2984	8701.8602	45.8665	−24.2527
	80	10 682.6048	8758.8185	45.0524	−25.8796
	86	10 727.9376	8932.1352	45.4329	−27.5181

NR framework as it should be. For neutral atoms, the relativistic part of shielding constant, meaning $\sigma^{R-NR} = \sigma^{t} - \sigma^{t,NR}$, contributes from 1% for Ne to 45% for Rn to the total σ. For ions these numbers are even higher because inner shells are more influenced by relativistic effects than outer shells.

Gaunt contributions to σ^{t} (meaning the difference in σ^{t} value calculated with and without Gaunt term included in SCF process) are also given in Tables III and IV. We observe that they grow in absolute values from higher to lower ionized atoms. Its values are the largest for neutral atoms.

We observe that Gaunt contributions to σ are not dependent on relativistic effects. They are $\approx -2\%$ of the relativistic effect for Ar and $\approx -0.3\%$ for Rn. The fact that the percentage of Gaunt contributions goes down when compared with relativistic effects on σ is related with the increase of relativistic effects. When σ^{Gaunt} is compared with σ^{NR} it is observed that $\sigma^{Gaunt} \approx -0.05\%$ of σ^{NR} for Ar and $\approx -0.27\%$ of σ^{NR} for Rn. Another interesting finding is that σ^{Gaunt} change its sign between

Be-like and Ne-like Rn and between He-like and Be-like Hg.

B. QED contributions for neutral atoms and ions

Tables V and VI collect QED contributions, calculated with model A, to σ^{ee} for selected atoms and their ions. The QED contributions, σ^{QED}, were splitted into parts according to particular types of e-e excitations: $1s \rightarrow 2s$ (only for He-like atomic systems), $1s \rightarrow ns$ ($n > 2$), $2s \rightarrow ns$, $3s \rightarrow ns$, and $4s \rightarrow ns$. We used three $C^{QED/DC}$ coefficients in present work: $C^{QED/DC}_{1s,2s}$, $C^{QED/DC}_{1s,ns}$ (assuming $\alpha \simeq \Delta\varepsilon^{QED}_{1s}/\varepsilon^{DC}_{1s}$ and $\beta \simeq \Delta\varepsilon^{VP}_{1s}/\varepsilon^{DC}_{1s}$), and $C^{QED/DC}_{2s,ns}$ (assuming $\alpha \simeq \Delta\varepsilon^{QED}_{2s}/\varepsilon^{DC}_{2s}$ and $\beta \simeq \Delta\varepsilon^{VP}_{2s}/\varepsilon^{DC}_{2s}$; used for $2s \rightarrow ns$, $3s \rightarrow ns$, and $4s \rightarrow ns$ excitations). With DIRAC code one can calculate both bounded and unbounded though discretized electronic orbitals, but we assume that QED effects on excitations from the inner orbitals to highly excited, bounded or unbounded though discretized orbitals are the same (QED effects arises from strong electric field near nucleus).

As stated before in Refs. 14 and 15, QED contributions to NMR shielding constants have negative sign. The σ^{QED} is almost independent of the number of electrons in ion. It is because a major part of e-e excitations occur from inner $1s$ and $2s$ shells, that are more influenced by QED effects. Even if contributions from $1s$ and $2s$ shells decrease a little with n_{el}, the contributions from $3s$ and $4s$ shells arise instead. As one can see from Tables V and VI, the σ^{QED} contributes to σ^t from -0.0011% for Ne to -0.51% for Rn. For neutral atoms σ^{QED} scales like Z^5, a dependence that is weaker than that of H-like atoms for which σ^{QED} scales like Z^4.[15]

QED effects contributes to σ^{R-NR} from -0.10% for Ne to -1.13% for Rn. Note that $\sigma^{QED}/\sigma^{R-NR}$ ratio grows almost linearly with Z for neutral atoms. The $\sigma^{QED}/\sigma^{R-NR}$ ratio depends also on the number of electrons; the higher the number of electrons in ion, the lower the ratio $\sigma^{QED}/\sigma^{R-NR}$. The contribution to σ of QED effects is larger than that of Gaunt for higher Z atoms. The $\sigma^{QED}/\sigma^{Gaunt}$ ratio depends on the number of electrons; the higher number of electrons in ion, the lower $\sigma^{QED}/\sigma^{Gaunt}$ ratio. For neutral atoms, the $\sigma^{QED}/\sigma^{Gaunt}$ ratio grows like $Z^{2.4}$.

In Table VII we present the contributions of QED effects to σ^{ee} for neutral atoms, calculated with model B. One can see that QED contributions from model B are about 79–97% of QED contributions from model A, except for Ne and Ar atoms. Results from the less accurate model B show that, by applying model A, we are getting reliable orders of magnitude for QED contributions to NMR shielding constants.

The percentage with which QED effects contribute to the total NMR shielding constants, σ^{QED}/σ^t, for neutral atoms (present work) and for H-like atomic systems (Yerokhin *et al.* work[15]) are presented on Fig. 2. The

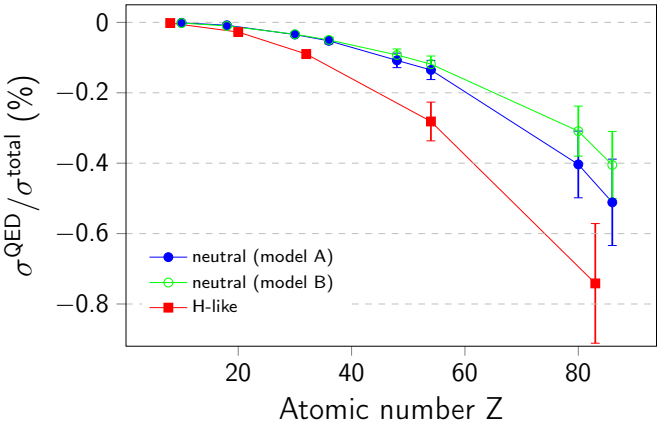

FIG. 2. Percentage of QED effects on total NMR shielding constants, σ^{QED}/σ^t (%).

analysis of uncertainty was performed in our previous paper[23].

In Figs. 3 and 4 we observe the pattern of dependence with Z of four terms that contribute to both, σ and the total energy. Such terms are: NR, relativistic, QED and Breit/Gaunt.

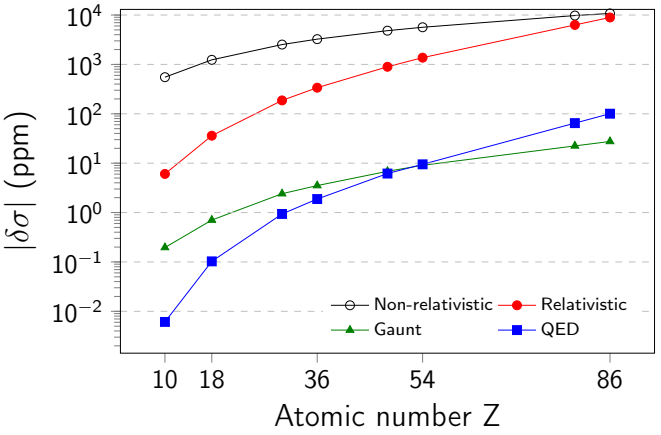

FIG. 3. Individual contributions (absolute values) to the nuclear shielding for selected atoms.

It is seen that, for σ, relativistic effects are as large as the NR shieldings when $Z \simeq 86$, though they are smaller when $Z \simeq 10$. On the other hand QED effects grow faster than all the other ones as Z grows. For $Z \simeq 86$ QED effects are less than two orders of magnitude smaller than both, relativistic and NR contributions. Hence, if one wants to reproduce NMR shieldings within less than 1% of error one must include QED effects.

In Fig. 4 we observe that, the contributions of QED effects and Breit interactions to the total atomic energy of atoms, grow together almost at the same rate. This behavior is different as that observed in Fig. 3, meaning that QED effects are larger for shieldings than for electronic energies of atoms. A similar behavior is also observed for relativistic effects, which are larger for shieldings than for

TABLE V. QED contributions to σ^{ee} (model A) for Ne, Ar, Zn, Kr, and Cd, and their ions.

		σ^{QED} (ppm)							
		$1s-2s$	$1s-ns$	$2s-ns$	$3s-ns$	$4s-ns$	total	σ^{QED}/σ^{t}	$\sigma^{QED}/\sigma^{R-NR}$
Z	n_{el}	exc.	exc.	exc.	exc.	exc.		(%)	(%)
10	2	−0.0006	−0.0051				−0.0057	−0.0016	−0.1148
	4		−0.0051	−0.0011			−0.0062	−0.0015	−0.1123
	10		−0.0052	−0.0009			−0.0061	−0.0011	−0.1026
18	2	−0.0124	−0.0814				−0.0938	−0.0143	−0.3285
	4		−0.0817	−0.0213			−0.1030	−0.0128	−0.3194
	10		−0.0834	−0.0182			−0.1016	−0.0088	−0.2918
	12		−0.0822	−0.0163	−0.0043		−0.1028	−0.0086	−0.2904
	18		−0.0826	−0.0167	−0.0035		−0.1027	−0.0081	−0.2862
30	2	−0.1210	−0.7189				−0.8399	−0.0702	−0.5905
	4		−0.7208	−0.2110			−0.9318	−0.0636	−0.5756
	10		−0.7303	−0.1924			−0.9227	−0.0429	−0.5251
	12		−0.7109	−0.1634	−0.0659		−0.9402	−0.0420	−0.5225
	18		−0.7150	−0.1641	−0.0594		−0.9385	−0.0380	−0.5118
	30		−0.7194	−0.1673	−0.0499	0.0000	−0.9366	−0.0346	−0.5011
36	2	−0.2630	−1.4243				−1.6873	−0.1108	−0.6607
	4		−1.4277	−0.4451			−1.8728	−0.1006	−0.6426
	10		−1.4445	−0.4128			−1.8573	−0.0684	−0.5868
	12		−1.3997	−0.3453	−0.1518		−1.8968	−0.0669	−0.5840
	18		−1.4071	−0.3459	−0.1402		−1.8933	−0.0604	−0.5713
	30		−1.4145	−0.3481	−0.1086		−1.8711	−0.0531	−0.5549
	36		−1.4163	−0.3500	−0.1117		−1.8780	−0.0524	−0.5530
48	2	−0.9093	−4.4783				−5.3875	−0.2284	−0.8093
	4		−4.4879	−1.5564			−6.0442	−0.2109	−0.7915
	10		−4.5346	−1.4745			−6.0091	−0.1472	−0.7242
	12		−4.3585	−1.2042	−0.5909		−6.1536	−0.1443	−0.7205
	18		−4.3794	−1.2048	−0.5606		−6.1449	−0.1302	−0.7041
	30		−4.3875	−1.1836	−0.4228	−0.1754	−6.1692	−0.1146	−0.6934
	36		−4.3940	−1.1893	−0.4275	−0.1603	−6.1712	−0.1114	−0.6892
	48		−4.4008	−1.1945	−0.4314	−0.1389	−6.1656	−0.1079	−0.6854

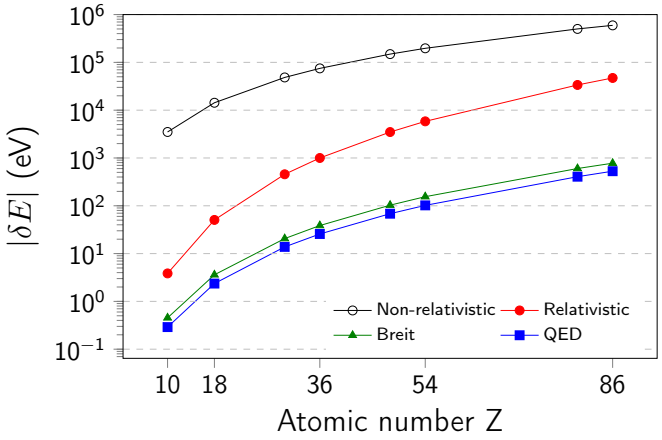

FIG. 4. Individual contributions (absolute values) to the total energy for selected atoms.

energies when compared with NR contributions in both cases.

C. QED contribution for diatomic halogen molecules

NMR shielding constants (without QED contributions, but employing a Dirac–Coulomb–Gaunt Hamiltonian) for Br, I, and At halogens nuclei in Br_2, I_2, and At_2 homonuclear molecules, and HBr, HI, and HAt heteronuclear molecules, and Br^-, I^-, and At^- ions are presented in Table VIII. Because of lack of spherical symmetry, the shielding tensor contributions parallel ($\parallel$) and perpendicular ($\perp$) to the molecular axis are presented. As one can see, $\sigma_{\parallel}^{ee}$ and $\sigma_{\perp}^{ee}$ differ from each other more than $\sigma_{\parallel}^{pp}$ and $\sigma_{\perp}^{pp}$. This can be understood by using a relativistic model that relates σ with the spin-rotation constants.[54–56] There are different contributions to the parallel and perpendicular components of the spin-rotation tensor caused by the change of electron density according to bond formation.

QED contributions to σ^{ee} are collected in Table IX. We performed calculations of Br^-, I^-, and At^- ions instead of the calculations of regular Br, I, and At atoms, because the DIRAC code has issues related with open-shell systems.

One can see in Table IX, that QED contributions to $\sigma(X)$ in X_2 molecules (X = Br, I, At) are little smaller

TABLE VI. Like Table V, but for Xe, Hg, and Rn, and their ions.

				σ^{QED} (ppm)					
3-8		$1s-2s$	$1s-ns$	$2s-ns$	$3s-ns$	$4s-ns$	total	σ^{QED}/σ^{t}	$\sigma^{QED}/\sigma^{R-NR}$
Z	n_{el}	exc.	exc.	exc.	exc.	exc.		(%)	(%)
54	2	−1.5292	−6.7793				−8.3084	−0.2858	−0.8300
	4		−6.7934	−2.4912			−9.2846	−0.2638	−0.8064
	10		−6.8621	−2.3769			−9.2390	−0.1875	−0.7389
	12		−6.5695	−1.9212	−0.9809		−9.4716	−0.1840	−0.7350
	18		−6.6000	−1.9222	−0.9382		−9.4604	−0.1664	−0.7181
	30		−6.5990	−1.8721	−0.7061	−0.3290	−9.5062	−0.1465	−0.7073
	36		−6.6108	−1.8804	−0.7113	−0.3075	−9.5100	−0.1422	−0.7027
	48		−6.6159	−1.8838	−0.7050	−0.2477	−9.4525	−0.1360	−0.6951
	54		−6.6226	−1.8881	−0.7107	−0.2582	−9.4796	−0.1352	−0.6917
80	2	−12.1398	−42.1905				−54.3303	−0.7407	−1.2058
	4		−42.2834	−20.8103			−63.0937	−0.7180	−1.1982
	10		−42.7113	−20.2322			−62.9435	−0.5602	−1.1021
	12		−40.1205	−15.6795	−9.1133		−64.9134	−0.5537	−1.0975
	18		−40.2977	−15.7083	−8.8875		−64.8934	−0.5120	−1.0722
	30		−39.9437	−14.9245	−6.6414	−3.9353	−65.4449	−0.4624	−1.0591
	36		−40.0215	−14.9743	−6.6628	−3.8336	−65.4922	−0.4495	−1.0510
	46		−40.1550	−15.0882	−6.6824	−3.5854	−65.5110	−0.4332	−1.0472
	60		−40.2419	−15.2391	−6.8101	−3.2923	−65.5833	−0.4178	−1.0441
	80		−40.1393	−15.0934	−6.6010	−2.9050	−64.7387	−0.4035	−1.0253
86	2	−20.9742	−63.7083				−84.6825	−0.9157	−1.3646
	4		−63.8550	−34.0958			−97.9508	−0.8842	−1.3438
	10		−64.5155	−33.2451			−97.7606	−0.7056	−1.2368
	12		−60.2874	−25.5057	−15.2115		−101.0046	−0.6989	−1.2325
	18		−60.5550	−25.5637	−14.8771		−100.9958	−0.6503	−1.2042
	30		−59.8948	−24.1817	−11.0859	−6.7802	−101.9426	−0.5931	−1.1907
	36		−60.0149	−24.2606	−11.1225	−6.6381	−102.0361	−0.5776	−1.1816
	46		−60.2194	−24.4409	−11.1519	−6.2544	−102.0666	−0.5579	−1.1775
	60		−60.3695	−24.6982	−11.3552	−5.7573	−102.1802	−0.5386	−1.1742
	80		−60.1529	−24.3805	−10.8917	−4.8929	−100.3180	−0.5160	−1.1453
	86		−60.1770	−24.4150	−10.9369	−4.9683	−100.4972	−0.5112	−1.1251

TABLE VII. QED contributions to σ^{ee} (model B) for Ne, Ar, Zn, Kr, Cd, Xe, Hg, and Rn. "B/A" means σ^{QED}(model B)/σ^{QED}(model A) ratio.

			σ^{QED} (ppm)					
2-6	$1s-ns$	$2s-ns$	$3s-ns$	$4s-ns$	total	σ^{QED}/σ^{t}	$\sigma^{QED}/\sigma^{R-NR}$	B/A
Z	exc.	exc.	exc.	exc.		(%)	(%)	(%)
10	−0.0096	−0.0007			−0.0103	−0.0018	−0.1726	168.3
18	−0.1130	−0.0151	−0.0010		−0.1292	−0.0101	−0.3598	125.7
30	−0.7534	−0.1380	−0.0199		−0.9114	−0.0336	−0.4877	97.3
36	−1.4480	−0.2905	−0.0506		−1.7890	−0.0499	−0.5268	95.3
48	−4.0903	−0.9478	−0.2198	−0.0302	−5.2881	−0.0926	−0.5878	85.8
54	−6.2914	−1.5565	−0.3960	−0.0712	−8.3151	−0.1186	−0.6067	87.7
80	−33.5908	−11.2176	−3.7581	−0.9958	−49.5623	−0.3089	−0.7850	76.6
86	−52.3454	−18.8301	−6.5755	−1.8721	−79.6231	−0.4050	−0.8914	79.2

than in the case of X^- ion. The $\sigma_{\parallel}^{QED}$ values for atoms in X_2 molecules are closer to σ^{QED} for ions than the $\sigma_{\perp}^{QED}$ values. Furthermore, $\sigma^{QED}(X)$ for X in HX molecules (X = Br, I, At) are closer to its atomic σ^{QED} values. It is worth to highlight the fact that σ^{ee} becomes more positive (diamagnetic) as relativistic effects increase. This is more pronounced for perpendicular contributions. We also found that the virtual ns → n's type excitations give a total contribution to σ^{ee} that is close to 95% (see Supplementary Information)

TABLE VIII. NMR shielding constants (without QED contributions, but with Gaunt term included) for Br_2, I_2, At_2, HBr, HI, and HAt molecules (per atom) and Br^-, I^-, and At^- ions. Between square brackets results of calculations with the Gauge origin at the position of the heavy nucleus are included. Shieldings are given in ppm and distance in pm.

	$d_{X\text{-}X}$	σ^t	σ^{pp}	σ^{ee}	$\sigma^t_\parallel$	$\sigma^{pp}_\parallel$	$\sigma^{ee}_\parallel$	$\sigma^t_\perp$	$\sigma^{pp}_\perp$	$\sigma^{ee}_\perp$
Br_2	228.11	2444.3800	2979.2262	−534.8462	3332.0085	2919.3630	412.6455	2000.5657	3009.1578	−1008.5920
		[2444.2677]								
Br^-		3436.6011	2912.5954	524.0057	3436.6011	2912.5954	524.0057	3436.6011	2912.5954	524.0057
HBr	141.45	2945.5229	2913.9614	31.5615	3390.5349	2912.0992	478.4357	2723.0169	2914.8924	−191.8756
		[2945.5189]								
I_2	266.63	5512.6072	4975.4177	537.1895	6309.3206	4893.7703	1415.5503	5114.2505	5016.2414	98.0091
		[5524.7590]								
I^-		6795.1202	4887.0379	1908.0823	6795.1202	4887.0379	1908.0823	6795.1202	4887.0379	1908.0823
HI	160.90	5857.8445	4887.6303	970.2142	6553.6279	4886.0641	1667.5637	5509.9528	4888.4133	621.5394
		[5857.8425]								
At_2	296.27	16 915.9043	8756.1722	8159.7321	15 623.7007	8639.6204	6984.0803	17 562.0062	8814.4481	8747.5581
At^-		19 162.2480	8627.9157	10 534.3322	19 162.2480	8627.9157	10 534.3322	19 162.2480	8627.9157	10 534.3322
HAt	171.17	18 146.9316	8627.5773	9519.3543	16 258.8652	8629.0506	7629.8146	19 090.9648	8626.8407	10 464.1241
		[18 146.9229]								

TABLE IX. QED contributions to σ^{ee} for Br_2, I_2, At_2, HBr, HI, and HAt molecules (per atom) and Br^-, I^-, and At^- ions.

		σ^{QED} (ppm)								
3-11		$\sigma^{QED}_\parallel$				$\sigma^{QED}_\perp$				σ^{QED}_{iso}
3-67-1011-11	$d_{X\text{-}X}$ (pm)	$1s-ns$	$2s-ns$	$3s-ns$	$4s-ns$	$1s-ns$	$2s-ns$	$3s-ns$	$4s-ns$	total
Br_2	228.11	−1.2663	−0.3199	−0.0962		−1.2412	−0.2506	−0.0977		−1.6205
Br^-		−1.2669	−0.3213	−0.1018		−1.2669	−0.3213	−0.1018		−1.6900
HBr	141.45	−1.2658	−0.3210	−0.1008		−1.2746	−0.3192	−0.0954		−1.6875
I_2	266.63	−6.1132	−1.7961	−0.6518	−0.1747	−6.0602	−1.6987	−0.5645	−0.2337	−8.6166
I^-		−6.1078	−1.8046	−0.6763	−0.2454	−6.1078	−1.8046	−0.6763	−0.2454	−8.8342
HI	160.90	−6.1010	−1.8020	−0.6707	−0.2326	−6.1480	−1.7974	−0.6578	−0.2110	−8.8063
At_2	296.27	−54.4513	−22.2530	−9.5767	−3.6524	−54.4016	−21.8176	−9.1525	−3.8709	−89.4729
At^-		−54.1502	−22.5061	−10.0639	−4.5892	−54.1502	−22.5061	−10.0639	−4.5892	−91.3093
HAt	171.17	−54.0260	−22.4104	−9.9144	−4.3066	−54.6905	−22.4272	−9.9199	−4.5336	−91.2666

IV. CONCLUSIONS

When searching for highly accurate atomic and molecular response properties one should consider physical effects that were taken to be vanishingly small few years ago. Among them one must include QED effects and Breit interactions.

As a next step in our research program that aims to include QED effects together with electron correlation on response properties in atoms and molecules, we present here two effective models that were developed to calculate QED effects on top of the paramagnetic-like contributions to the NMR magnetic shieldings of nuclei in many-electron atoms and diatomic molecules. Our results are based on state-of-the-art calculations of QED effects on H-like systems, taken from the works of Yerokhin and collaborators.[14,15]

One of our most important findings is related with new insights about the likely physical origin of the paramagnetic-like or ee contribution, and the diamagnetic-like or pp contribution to the magnetic shieldings, within a relativistic framework. The analysis of the physical mechanisms that are involved in them shows that pp contributions can be rationalized as due to virtual electron-positron pair creation/annihilation in such a way that: i) for a given atomic number Z, each subshell contributes almost the same value, being the condition for doing it that ii) the subshell be occupied. On the other side, the ee contributions can be understood as mostly due to virtual excitations that start from linear combinations of s-type gaussian-type orbitals and do not depend on n_{el}.

Another important finding is the fact that QED corrections to the NMR shielding constant of many-electron systems can be close or even larger than 1% of the relativistic correction for high-Z atoms. On the other hand its Z dependence is proportional to Z^5, being proportional to Z^4 for H-like systems. Furthermore, $\sigma^{QED}/\sigma^{R-NR} \propto Z$. It is worth to mention that QED effects are larger on ions than on neutral atoms for a fixed Z.

We also found that, for molecules, most of the main ee excitations involved in the relativistic shielding calculations occur between the lowest molecular orbitals (which are similar to $1s$ and $2s$ atomic orbitals) and higher unoc-

cupied orbitals. This behavior is also found in the main mechanisms contributing to σ^{QED}. So, its origin is highly atomic for magnetic shieldings in molecules and this is the reason why we were able to apply our models to them.

We have calculated relativistic, non-relativistic, Breit (or a fraction of the total Gaunt) and QED contributions to the shieldings of the following atomic and molecular systems: atoms with $10 \leq Z \leq 86$ and their ionic closed-shell electronic structures, and X_2 and HX (X = Br, I, At) molecules. The Z dependence of those contributions to both, the magnetic shielding constant and the total atomic energy are such that the magnetic shielding constants are more influenced by relativistic and QED effects than the total atomic energies.

At the moment we are trying to extend the application of our models to the NMR J-couplings. We now know that the $C_K(\frac{DCBV}{DCB})$ factor is larger than the $C_B(\frac{DCBV}{DCB})$ factor. Thus we expect that QED corrections to J-coupling constants should be larger, or at least of the same size, as QED corrections to NMR shielding constants.

SUPPLEMENTARY MATERIAL

We introduce some supplemental material in few tables. In tables 1, 2, 3, and 4 we show the pattern of contributing excitations (ia) that start in each of the four lowest occupied MO, to the parallel component of the e-e terms of the shielding of iodine nucleus in I_2, *e.g.*, $\sigma_{\parallel}^{(e-e)}(\mathrm{I};\mathrm{I}_2)$. The pattern for perpendicular components are similar. We include only contributions that are larger than a very small threeshold.

In tables 5 and 6 we show results of the influence, on shielding calculations, due to different Gauge-origins and basis sets.

ACKNOWLEDGEMENTS

K. K. was supported by the Argentinian National Research Council for Science and Technology (CONICET), by resolution No. 8221/15. We acknowledge support from CONICET by grant PIP 112-20130100361 and FONCYT by grant PICT 2016-2936.

[1] M. Kaupp, M. Bühl, and V. G. Malkin, eds., *Calculation of NMR and EPR Parameters: Theory and Applications* (Wiley-VCH, Weinheim, 2004).
[2] J. Vaara, Phys. Chem. Chem. Phys. **9**, 5399 (2007).
[3] R. H. Contreras, ed., *High Resolution NMR Spectroscopy. Understanding Molecules and their Electronic Structures*, Science and Technology of Atomic, Molecular, Condensed Matter & Biological Systems (Elsevier, 2013).
[4] Y. Y. Rusakov and L. B. Krivdin, Russ. Chem. Rev. **82**, 99 (2013).
[5] L. Visscher, T. Enevoldsen, T. Saue, H. J. A. Jensen, and J. Oddershede, J. Comput. Chem. **20**, 1262 (1999).
[6] G. A. Aucar, R. H. Romero, and A. F. Maldonado, Int. Rev. Phys. Chem. **29**, 1 (2010).
[7] I. A. Aucar, C. A. Giménez, and G. A. Aucar, RSC Adv. **8**, 20234 (2018).
[8] D. Andrae, "Nuclear Charge Density and Magnetization Distributions," in *Handbook of Relativistic Quantum Chemistry*, edited by W. Liu (Springer Berlin Heidelberg, Berlin, Heidelberg, 2017) pp. 51–81.
[9] P. Indelicato and P. J. Mohr, "Introduction to Bound-State Quantum Electrodynamics," in *Handbook of Relativistic Quantum Chemistry*, edited by W. Liu (Springer Berlin Heidelberg, Berlin, Heidelberg, 2017) pp. 131–243.
[10] A. F. Maldonado, C. A. Giménez, and G. A. Aucar, J. Chem. Phys. **136**, 224110 (2012).
[11] R. H. Romero and G. A. Aucar, Int. J. Mol. Sci. **3**, 914 (2002).
[12] R. H. Romero and G. A. Aucar, Phys. Rev. A: At. Mol. Opt. Phys. **65**, 053411 (2002).
[13] A. Rudziński, M. Puchalski, K. Pachucki, A. Rudziński, M. Puchalski, and K. Pachucki, J. Chem. Phys. **130**, 244102 (2009).
[14] V. A. Yerokhin, K. Pachucki, Z. Harman, and C. H. Keitel, Phys. Rev. Lett. **107**, 043004 (2011).
[15] V. A. Yerokhin, K. Pachucki, Z. Harman, and C. H. Keitel, Phys. Rev. A: At. Mol. Opt. Phys. **85**, 22512 (2012).
[16] P. Pyykkö and L.-B. Zhao, J. Phys. B: At., Mol. Opt. Phys. **36**, 1469 (2003).
[17] V. M. Shabaev, Phys. Rep. **356**, 119 (2002).
[18] I. Lindgren, S. Salomonson, and B. Åsén, Phys. Rep. **389**, 161 (2004).
[19] K. G. Dyall, J. Chem. Phys. **139**, 021103 (2013).
[20] I. Lindgren and P. Indelicato, "Unifying Many-Body Perturbation Theory with Quantum Electrodynamics," in *Handbook of Relativistic Quantum Chemistry*, edited by W. Liu (Springer Berlin Heidelberg, Berlin, Heidelberg, 2017) pp. 313–341.
[21] V. M. Shabaev, I. I. Tupitsyn, and V. A. Yerokhin, Comput. Phys. Commun. **223**, 69 (2018).
[22] G. A. Aucar, Phys. Chem. Chem. Phys. **16**, 4420 (2014).
[23] C. A. Giménez, K. Kozioł, and G. A. Aucar, Phys. Rev. A: At. Mol. Opt. Phys. **93**, 032504 (2016).
[24] J. A. Lowe, C. T. Chantler, and I. P. Grant, Radiat. Phys. Chem. **85**, 118 (2013).
[25] K. Kozioł, C. A. Giménez, and G. A. Aucar, J. Chem. Phys. **148**, 044113 (2018).
[26] M. Kubiszewski, W. Makulski, and K. Jackowski, J. Mol. Struct. **737**, 7 (2005).
[27] K. Jackowski, M. Jaszuński, and M. Wilczek, J. Phys. Chem. A **114**, 2471 (2010).
[28] M. Jaszuński, A. Antušek, P. Garbacz, K. Jackowski, W. Makulski, and M. Wilczek, Prog. Nucl. Magn. Reson. Spectrosc. **67**, 49 (2012).
[29] B. Adrjan, W. Makulski, K. Jackowski, T. B. Demissie, K. Ruud, A. Antušek, and M. Jaszuński, Phys. Chem. Chem. Phys. **18**, 16483 (2016).
[30] G. A. Aucar, T. Saue, L. Visscher, and H. J. A. Jensen, J. Chem. Phys. **110**, 6208 (1999).
[31] T. Saue and H. J. A. Jensen, J. Chem. Phys. **118**, 522 (2003).
[32] E. A. Moore, Mol. Phys. **97**, 375 (1999).
[33] N. C. Pyper, Mol. Phys. **97**, 381 (1999).
[34] W. R. Johnson and G. Soff, At. Data Nucl. Data Tables **33**, 405 (1985).
[35] K. Kozioł and G. A. Aucar, J. Chem. Phys. **148**, 134101 (2018).
[36] H. A. Bethe, Phys. Rev. **72**, 339 (1947).
[37] P. Indelicato and J. Desclaux, Mcdfgme, a multiconfiguration Dirac-Fock and General Matrix Elements program (release 2005); http://dirac.spectro.jussieu.fr/mcdf.
[38] J. P. Desclaux, Comput. Phys. Commun. **35**, C (1984).
[39] I. P. Grant, *Relativistic Quantum Theory of Atoms and Molecules*, edited by I. P. Grant, Springer Series on Atomic, Optical, and Plasma Physics, Vol. 40 (Springer, New York, NY, 2007).
[40] O. Gorceix, P. Indelicato, and J.-P. Desclaux, Journal of Physics B: Atomic and Molecular Physics **20**, 639 (1987).
[41] G. Breit, Physical Review **34**, 553 (1929).
[42] E. A. Uehling, Physical Review **48**, 55 (1935).
[43] L. W. Fullerton and G. A. Rinker, Physical Review A **13**, 1283 (1976).

[44]DIRAC, a relativistic ab initio electronic structure program, Release DIRAC17 (2017), written by L. Visscher, H. J. Aa. Jensen, R. Bast, and T. Saue, with contributions from V. Bakken, K. G. Dyall, S. Dubillard, U. Ekström, E. Eliav, T. Enevoldsen, E. Faßhauer, T. Fleig, O. Fossgaard, A. S. P. Gomes, E. D. Hedegård, T. Helgaker, J. Henriksson, M. Iliaš, Ch. R. Jacob, S. Knecht, S. Komorovský, O. Kullie, J. K. Lærdahl, C. V. Larsen, Y. S. Lee, H. S. Nataraj, M. K. Nayak, P. Norman, G. Olejniczak, J. Olsen, J. M. H. Olsen, Y. C. Park, J. K. Pedersen, M. Pernpointner, R. di Remigio, K. Ruud, P. Sałek, B. Schimmelpfennig, A. Shee, J. Sikkema, A. J. Thorvaldsen, J. Thyssen, J. van Stralen, S. Villaume, O. Visser, T. Winther, and S. Yamamoto (see http://www.diracprogram.org).
[45]L. Visscher and K. G. Dyall, At. Data Nucl. Data Tables **67**, 207 (1997).
[46]K. G. Dyall, Theor. Chem. Acc. **135**, 128 (2016).
[47]K. G. Dyall, Theor. Chem. Acc. **115**, 441 (2006).
[48]K. G. Dyall and A. S. P. Gomes, "unpublished,".
[49]K. G. Dyall, Theor. Chem. Acc. **117**, 483 (2007).
[50]K. G. Dyall, Theor. Chem. Acc. **112**, 403 (2004).
[51]W. M. Haynes, *CRC Handbook of Chemistry and Physics, 97th Edition* (CRC Press, 2016).
[52]W. E. Lamb, Physical Review **60**, 817 (1941).
[53]T. Helgaker, M. Jaszuński, and K. Ruud, Chemical Reviews **99**, 293 (1999).
[54]W. H. Flygare, Chem. Rev. **74**, 653 (1974).
[55]I. A. Aucar, S. S. Gomez, C. G. Giribet, and G. A. Aucar, Phys. Chem. Chem. Phys. **18**, 23572 (2016).
[56]I. A. Aucar, S. S. Gomez, C. G. Giribet, and G. A. Aucar, J. Phys. Chem. Lett. **7**, 5188 (2016).